

**A SYNERGISTIC NANOSCALE ZERO VALENT IRON–HYDROGEN  
PEROXIDE TECHNOLOGY FOR TREATMENT OF INSENSITIVE  
MUNITIONS WASTEWATERS**

by

Oluwasegun Elijah Akanbi

A thesis submitted to the Faculty of the University of Delaware in partial fulfillment of the requirements for the degree of Master of Civil Engineering

Spring 2021

© 2021 Oluwasegun Elijah Akanbi

All Rights Reserved

**A SYNERGISTIC NANOSCALE ZERO VALENT IRON–HYDROGEN  
PEROXIDE TECHNOLOGY FOR TREATMENT OF INSENSITIVE  
MUNITIONS WASTEWATERS**

by

Oluwasegun Elijah Akanbi

Approved: \_\_\_\_\_  
Pei C. Chiu, Ph.D.  
Professor in charge of thesis on behalf of the Advisory Committee

Approved: \_\_\_\_\_  
Jack A. Puleo, Ph.D.  
Chair of the Department of Civil and Environmental Engineering

Approved: \_\_\_\_\_  
Levi T. Thompson, Ph.D.  
Dean of the College of Engineering

Approved: \_\_\_\_\_  
Louis F. Rossi, Ph.D.  
Vice Provost for Graduate and Professional Education and  
Dean of the Graduate College

## **ACKNOWLEDGMENTS**

I want to thank my adviser, Dr. Pei Chiu, for his guidance, insights, and support all through my master's program and during this study. I also want to thank Dr. Daniel Cha, my co-adviser on this research project, for his insights and suggestions. My appreciation also goes to Inyoung Kim and Kimberly Brogan who worked with me on this project. Many thanks to members of Dr. Chiu's Research Group for their support throughout my master's program. Special thanks to Jeffrey Hudson and other members of Chin's group for letting me use their TOC Analyzer instrument, again and again.

I would also like to acknowledge some staff of the Department of Civil and Environmental Engineering, University of Delaware, for their immense support during my program. Thanks to Dr. Yu Han Yu, Chris Reoli, Michael Davidson and Christine Murray.

Thanks to my friends and family, Adetayo and Toluwanimi Babarinde; Adeyinka and Babatunde Adebisi, for their love, prayers, and support throughout my program.

Lastly, I want to thank the Environmental Security Technology Certification Program (ESTCP) – Project ER18-5049, for funding me for my master's program and this study.

## TABLE OF CONTENTS

LIST OF FIGURES .....	v
ABSTRACT .....	viii
Chapter	
1 INTRODUCTION .....	1
2 LITERATURE REVIEW .....	3
3 METHODOLOGY .....	7
3.1 Materials .....	7
3.2 IMC Reduction with nZVI .....	7
3.3 Sequential Reduction and Oxidation of Individual IMCs .....	8
3.4 Sequential Reduction and Oxidation of Synthetic Wastewater .....	9
3.5 Analytical Methods .....	10
4 RESULTS AND DISCUSSIONS .....	12
4.1 IMC Reduction by nZVI .....	12
4.2 TOC and Nitrogen Products .....	21
4.3 Sequential Reduction and Oxidation of Synthetic Wastewater .....	24
5 PILOT SCALE STUDY .....	28
5.1 Relevance .....	28
5.2 Pilot Scale Study: Methodology .....	28
5.3 Pilot Scale Study: Results .....	29
6 CONCLUSION AND FUTURE RESEARCH .....	34
REFERENCES .....	36
Appendix	
SUPPLEMENTARY FIGURES .....	42

## LIST OF FIGURES

Figure 4.1	Concentrations of NTO, DNAN, and NQ during reduction by 30 mg of nZVI. All three MCs were in same reactor at an equal initial concentration of 0.5 mM. The solution volume was 40 mL. The pH was $2.0\pm 0.4$ . Error bars are based on duplicate reactors. ....	15
Figure 4.2	Concentrations of NTO, DNAN, and NQ 10 min after reduction by 30, 60, and 120 mg of nZVI. All three MCs were in same reactor at an equal initial concentration of 0.5 mM. The solution volume was 40 mL. The pH was $2.0\pm 0.4$ . Error bars are based on duplicate reactors.....	16
Figure 4.3	Disappearance of NTO and formation of its reduction product, following addition of 28.1 mg of Nanofer STAR. The initial concentration was 0.5 mM. Solution pH was constant at $2.0\pm 0.4$ . Error bars are based on duplicate reactors. ....	19
Figure 4.4	Disappearance of DNAN and formation of its reduction products, following addition of 28.1 mg of Nanofer STAR. The initial concentration was 0.5 mM. Solution pH was constant at $2.0\pm 0.4$ . Error bars are based on duplicate reactors. ....	20
Figure 4.5	Disappearance of NQ following addition of 28.1 mg of Nanofer STAR. The reduction product(s) of NQ was not identified. The initial concentration was 0.5 mM. Solution pH was constant at $2.0\pm 0.4$ . Error bars are based on duplicate reactors. ....	21
Figure 4.6	Concentrations of TOC in solutions containing individual MCs before reduction (Ctrl), after reduction (Aft. Red), and after oxidation (Aft. Oxi.). Reaction times were 10 min for reduction and 20 min for oxidation. pH was $2.0\pm 0.3$ for all solutions. Error bars are based on duplicate reactors.....	23

Figure 4.7	Concentrations of TNb in solutions containing individual MCs before reduction (Ctrl), after reduction (Aft. Red), and after oxidation (Aft. Oxi.). Reaction times were 10 min for reduction and 20 min for oxidation. pH was $2.0\pm 0.3$ for all solutions. Error bars are based on duplicate reactors.....	24
Figure 4.8	Concentrations of TOC in synthetic wastewater containing DNAN, NTO and NQ before reduction (Control), after reduction, and after oxidation. Reaction times were 10 min for reduction and 20 min for oxidation. pH was constant at $2.0\pm 0.3$ . Error bars are based on duplicate reactors.....	26
Figure 4.9	Concentrations of TNb in synthetic wastewater containing DNAN, NTO and NQ before reduction (Control), after reduction, and after oxidation. Reaction times were 10 min for reduction and 20 min for oxidation. pH was constant at $2.0\pm 0.3$ . Error bars are based on duplicate reactors.....	27
Figure 5.1	Schematic of Set-up for Pilot Scale Study Experiments .....	29
Figure 5.2	Disappearance of NTO and formation of its reduction product, ATO, with 2.0 g/L of Nanofer STAR at Pilot Scale. The initial concentration was 1.60 mM. Solution pH was constant at $2.0\pm 0.1$ . .....	30
Figure 5.3	Disappearance of DNAN and formation of its reduction products, with 1.2 g/L of Nanofer STAR at Pilot Scale. The initial DNAN concentration was 0.5 mM. Solution pH was constant at $2.0\pm 0.1$ . .....	31
Figure 5.4	Disappearance of NQ, with 2.0 g/L of Nanofer STAR at Pilot Scale. The initial NQ concentration was 2.5 mM. Solution pH was constant at $2.0\pm 0.2$ . .....	32
Figure 5.5	Concentrations of TOC in solutions containing individual MCs with Experiments at Pilot Scale before reduction (Control), after reduction (After Reduction), and after oxidation (After Oxidation). Reaction times were 30 min for reduction and 20 min for oxidation. pH was $2.4\pm 0.1$ for all solutions.....	33
Figure A1	Structures of the insensitive munitions compounds- NTO, DNAN, and NQ. The molecular masses of NTO, DNAN, and NQ are 130.06, 198.13, and 104.07 g/mol, respectively.....	42

Figure A2	Control (no nZVI) for reduction experiments. Solution volume was 40 mL, pH was $2.0\pm 0.4$ , and initial concentration of each MC was 0.5 mM. ....	43
Figure A3	Concentrations of MCs in synthetic wastewater before (control, magenta) and after (blue) Fenton oxidation. Solution volume was 30 mL. $\text{FeSO}_4$ and $\text{H}_2\text{O}_2$ were added to give initial aqueous Fe(II) and $\text{H}_2\text{O}_2$ concentrations of 42 mM and 84 mM, respectively. Reaction time was 20 min and pH was $2.0\pm 0.4$ . Error bars are based on duplicate reactors.....	44
Figure A4	Aqueous Fe(II) and Fe(III) concentrations after reduction and oxidation of three MCs individually. Reaction times were 10 min for reduction and 20 min for oxidation. pH was $2.0\pm 0.4$ . Error bars are based on duplicate reactors. Visible precipitates were observed in some reactors after oxidation, which will be Fe(III)-minerals. This would affect the actual amount of aqueous Fe(III) in solution after oxidation.....	45
Figure A5	DNAN (0.5 mM), NTO (1.75 mM), and NQ (3.5 mM) and their reduction products (DAAN and ATO, green bars) in synthetic wastewater before reduction (Ctrl), after reduction by nZVI (Aft. Red.), and after oxidation following $\text{H}_2\text{O}_2$ addition (Aft. Oxi.). pH was $2.0\pm 0.4$ . Error bars are based on duplicate reactors. ....	46

## ABSTRACT

The U.S. Army is phasing out legacy munitions compounds that are prone to accidental detonation and replacing them with insensitive munitions compounds (IMCs). The major IMCs, namely 3-nitro-1,2,4-triazol-5-one (NTO), 2,4-dinitroanisole (DNAN), and nitroguanidine (NQ), are not compatible with existing munitions wastewater treatment technologies such as granular activated carbon due to their high water solubilities. In this study, a two-stage process employing nanoscale zero-valent iron (nZVI) and hydrogen peroxide ( $H_2O_2$ ) was evaluated as a potential technology for destructive treatment of IMC wastewater. In the first stage, nZVI rapidly and completely degraded all three IMCs and generated dissolved Fe(II). NTO and DNAN were degraded via nitro reduction to 3-amino-1,2,4-triazol-5-one and 2,4-diaminoanisole, respectively. In the second stage,  $H_2O_2$  was added to oxidize the IMC reduction products through Fenton reaction. nZVI-treated NTO and DNAN samples showed 66% and 63% TOC removal, respectively, after oxidation. In contrast, NQ reduction products exhibited negligible mineralization. The results with individual IMCs were confirmed through an experiment using a synthetic wastewater containing all three IMCs (TOC = 42 mg/L per IMC). Furthermore, a 50-fold scale-up of the reactor size and volume in a pilot study to demonstrate the use of the technology at military facilities showed results consistent with those at smaller scales. This study illustrates the potential feasibility of an nZVI- $H_2O_2$  technology for treating IMC-laden wastewaters at military facilities.

## Chapter 1

### INTRODUCTION

The US Army is phasing out conventional munitions compounds and replacing them with insensitive munitions compounds (IMCs) that are thermally more stable and less sensitive to external stimuli (Isler, 1998; Davies and Provasas, 2006). The IMCs are manufactured for new insensitive munitions (IM) formulations such as IMX-101, which consists of 3-nitro-1,2,4-triazol-5-one (NTO), nitroguanidine (NQ) and 2,4-dinitroanisole (DNAN), and IMX-104, which consists of 1,3,5-trinitro-1,3,5-triazine (RDX), NTO, and DNAN (Cheng, 2014). With increase in military production and usage of these IMX formulations, the potential release of IM constituents to the environment may pose a growing concern since these compounds have been shown to be toxic or mutagenic to various organisms (Crouse et al., 2015; Johnson et al., 2017; Guilherme et al., 2018; Madeira et al., 2018). Effective treatment of IMX production wastewaters is necessary to remove these potentially harmful IMCs, thereby minimizing the risk of environmental contamination and ecological impact.

However, existing treatment processes for traditional munitions wastewater are not compatible with IMX production wastewater due to the unique properties of IMCs (Felt et al., 2013). For example, adsorption with granular activated carbon (GAC) is commonly used for the treatment of wastewaters at manufacturing and production facilities. While effective in removing legacy munitions compounds, e.g., 2,4,6-trinitrotoluene (TNT) and RDX, that are rather insoluble and hydrophobic, GAC is ineffective in removing IMCs such as NTO and NQ due to their high water solubilities

and low octanol-water partitioning coefficients ( $K_{ow}$ ) (Spear et al., 1989; Dave et al., 2000; Sokkalingam et al., 2008; Felt et al., 2013). As a result, significantly larger quantities of GAC are required to treat IM waste streams in order to prevent rapid breakthrough. This challenge is further exacerbated by the much higher concentrations of IMCs in IMX wastewaters than those of TNT and RDX. Moreover, because the process is non-destructive, IMC-laden spent GAC needs to be transported off-site for proper treatment or disposal as hazardous wastes. Hence, these challenges not only adversely impact IMX production but result in additional labor, material, and disposal costs, as well as potential secondary contamination and liability.

In this study, batch experiments were performed to evaluate a synergistic, two-stage process that consists of IMC reduction by nanoscale zero-valent-iron (nZVI) and Fenton oxidation through hydrogen peroxide ( $H_2O_2$ ) addition, to completely destroy IM constituents in munitions production wastewaters. In the first stage, nZVI (aggregates of 25-nm nanoparticles, geometric area-to-mass ratio  $\approx 30,000 \text{ m}^2/\text{kg}$ ) was added to degrade the IMCs (DNAN, NTO, and NQ) through reduction. Concurrently, nZVI was oxidized to dissolved Fe(II). The Fe(II) was then used to activate  $H_2O_2$  added in the second stage, where reduction products of IMCs were mineralized through Fenton oxidation. Total organic carbon (TOC) and total bound nitrogen (TNb, or non-gaseous nitrogen) concentrations were used to assess the extent of IMC mineralization by the nZVI- $H_2O_2$  treatment.

## Chapter 2

### LITERATURE REVIEW

Many chemical and biological processes have been investigated as potential treatment alternatives to GAC for munitions wastewater containing IM constituents (Perreault et al., 2012; Felt et al., 2013; Fida et al., 2014; Richard and Weidhaas, 2014; Madeira et al., 2017; Chew et al., 2018; Terracciano et al., 2018). While some were able to remove one or two IMCs, none of them were effective in removing all IM compounds. Alkaline hydrolysis of DNAN has been evaluated in laboratory treatability studies, but the process could not remove NTO in IMX wastewater (Felt et al., 2013). Oxidative processes such as biological and chemical oxidation have been shown to remove DNAN and NTO (Gent et al., 2013; Terracciano et al., 2018), but they could not remove NQ (Gent et al., 2013). Several studies showed microbial degradation of NTO, NQ, and DNAN, suggesting biological treatment may be a viable option (Platten et al., 2010; Perreault et al., 2012; Fida et al., 2014; Krzmarzick et al., 2015; Indest et al., 2017; Madeira et al., 2017; Madeira et al., 2019). NTO could be microbially transformed to 3-amino-1,2,4-triazol-5-one (ATO) by mixed cultures under anaerobic conditions (Krzmarzick et al., 2015; Indest et al., 2017; Madeira et al., 2017). Madeira et al. (2019) reported that ATO was readily mineralized to CO<sub>2</sub>, N<sub>2</sub>, and NH<sub>4</sub><sup>+</sup> under aerobic conditions. These authors suggested a sequential anaerobic-aerobic approach for complete destruction of NTO (Madeira et al., 2017). Similarly, DNAN was transformed to 2,4-diaminoanisole (DAAN) in anaerobic fluidized bed bioreactors with ethanol as an electron donor (Platten et al., 2010). Olivares et al.

(2016) reported microbial transformation of DNAN to 2-methoxy-5-nitroanisole and DAAN under anaerobic conditions, but no DNAN transformation was observed under aerobic conditions. Biodegradation of NQ by pure and mixed cultures has been reported under both aerobic and anaerobic conditions (Kaplan et al., 1982; Perreault et al., 2012). However, biological processes were slow and required multiple days to completely transform NQ.

ZVI technology has been used in recent decades for the degradation of environmental contaminants, both as micro-size ZVI and as nano-sized particles (nZVI) (Matheson et al., 1994; Lowry et al., 2004; Mu et al., 2004; Lin et al., 2013; Bae et al., 2015). (n)ZVI has been proven to degrade a wide range of contaminants (Matheson et al., 1994; Roberts et al., 1996; Kim et al., 2000; Jiang et al., 2011; Lin et al., 2013; Xu et al., 2019). It has been shown to degrade chlorinated compounds, both aliphatic and aromatic chlorinated compounds, such as perchloroethylene (Roberts et al., 1996) and pentachlorophenol (Kim et al., 2000), respectively. Inorganic contaminants like nitrate have been shown to be reduced by (n)ZVI to ammonia (Cheng et al., 1997; Xu et al., 2019). (n)ZVI has been used in the removal of arsenic (III), a heavy metal, from groundwater (Kanel et al., 2005). (n)ZVI has also been shown to reduce nitroaromatics such as nitrobenzene, (Mu et al., 2004; Keum et al., 2004) and azo compounds such as azobenzene (Ye et al., 2006), with the production of the amino daughter product, aniline, as the final product in each case (Mu et al., 2004; Ye et al., 2006).

Specifically, (n)ZVI has been applied to the degradation of legacy munition compounds. Studies have shown that the legacy explosives TNT, RDX, and octahydro-1,3,5,7-tetranitro-1,3,5,7-tetrazocine (HMX) can be rapidly reduced by

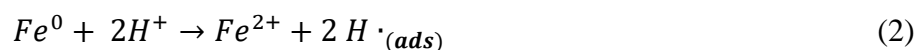
ZVI (Devlin et al., 1998; Singh et al., 1998; Oh et al., 2002; Oh et al., 2003; Oh et al., 2004). ZVI pretreatment of wastewater containing nitro explosives or azo dyes has been shown to increase the rate and extent of mineralization of these aerobically refractory compounds in subsequent biological or chemical oxidation processes (Perey et al., 2002; Oh et al., 2003). Ahn et al. (2014) reported ZVI treatment transformed DNAN in munitions wastewater into products that were more amenable to biological oxidation.

(n)ZVI reduction of contaminants, under anoxic conditions, has been known to be predominantly via one of two mechanisms: (1) electron transfer (Cheng et al., 1997; Mu et al., 2004) or (2) hydrogen atom transfer (Mu et al., 2004; Ye et al., 2006). Studies have also shown a third mechanism, (3) Surface-bound Fe(II) on iron-oxide, where aqueous Fe(II) ( $Fe(II)_{(aq)}$ ) produced from corrosion of (n)ZVI, reacts with the iron-oxide coating covering portions of the (n)ZVI at the time, thus, forming a reactive surface (Bae et al., 2015). However, mechanism (3) is only possible at high or circumneutral pH, which allows the formation of stable iron oxides on the (n)ZVI surface.

(n)ZVI as an electron donor in mechanism (1) follows the half-reaction shown in Eq. 1:



In mechanism (2), the electrons are accepted by protons which are then reduced to hydrogen atoms, a reactive species, which reacts with the target compound(s). Eq. 2 shows the formation of the reactive hydrogen species.



(n)ZVI has, thus, been known to be an effective agent for contaminant degradation, including munitions contaminants.

To date, however, ZVI has not been evaluated against NTO and NQ, which may exhibit different reactivities toward ZVI than their nitroaromatic counterparts, DNAN and TNT. In addition, reactivity of ZVI is often limited by its geometric area-to-mass ratio (ca.  $0.9 \text{ m}^2/\text{kg}$  for a 1 mm particle) which may render it slow and infeasible for treating wastewaters containing high concentrations of NTO and NQ.

Fenton oxidation, the most common advanced oxidation process for the treatment of organic contaminants because of its simplicity and non-selectivity (Huang et al., 1993), was also applied in this study, as a second step in the treatment process.

This study focuses on evaluation of a potential two-staged nZVI- $\text{H}_2\text{O}_2$  technology for treating munitions wastewaters laden with IMCs. Here, the application of nZVI to three major IMCs is studied. This is the first time nZVI reaction with NTO and NQ has been studied. Also, Fenton oxidation of the reduction products, in the second stage of the treatment, was evaluated. The dissolved Fe(II) produced from the concurrent oxidation of nZVI in the first stage, was utilized on addition of  $\text{H}_2\text{O}_2$ , for Fenton oxidation in the second stage.

## Chapter 3

### METHODOLOGY

#### 3.1 Materials

Nanofer STAR, an air-stable nZVI product was purchased from Nano Iron, s.r.o. (Czech Republic). The oxide-coated nZVI powder had an Fe(0) content of 65–80%, a magnetite ( $\text{Fe}_3\text{O}_4$ ) content of 20–35%, and a specific surface area of  $>25 \text{ m}^2/\text{g}$ , according to the vendor (Nano Iron, 2018). NQ and DNAN were obtained from Sigma-Aldrich (St. Louis, MO). NTO was provided by Picatinny Arsenal, NJ. Hydrogen peroxide (30%) and sulfuric acid ( $\text{H}_2\text{SO}_4$ , 98%) were purchased from Fisher Scientific (Waltham, MA). The structures and molecular formula of the three IMCs are shown in Figure A1. Trifluoroacetic acid (TFA), acetonitrile ( $\geq 99.9\%$ ), and methanol ( $\geq 99.9\%$ ) were purchased from Sigma-Aldrich (St. Louis, MO). All munitions compound (MC) solutions were prepared in a mineral salt medium containing the following ions to mimic the ion composition of IMX wastewater (Kim et al., 2019): 0.05 mM KCl, 4.9 mM NaCl, 1.3 mM  $\text{CaSO}_4$ , and 0.8 mM  $\text{MgSO}_4$ . All chemicals used in the mineral salt medium were purchased from Acros Organics (Fair Lawn, NJ) and used as received.

#### 3.2 IMC Reduction with nZVI

All experiments were carried out in an anaerobic glove box under  $\text{N}_2$  (98%) and  $\text{H}_2$  (2%) (Coy, Grass Lake, MI) at room temperature. Sixty-mL amber borosilicate

vials were used as batch reactors and prepared in duplicates. Each reactor was filled with 40 mL of deoxygenated IM solution containing 0.5 mM each of DNAN, NTO, and NQ. The initial pH was adjusted to  $2.0 \pm 0.4$  with concentrated sulfuric acid to mimic the low pH of IMX wastewaters (Felt et al., 2013) due to NTO deprotonation ( $pK_a$  3.76). Reactors were placed on an end-over-end shaker at 40 rpm, and 30 mg of nZVI powder was added to initiate reaction. At different elapsed times, aliquots of solution were withdrawn and immediately passed through a 0.22- $\mu$ m PTFE syringe filter to remove nZVI particles and stop further reaction. For comparison, experiments were also performed with individual IM compounds. These experiments were conducted under identical conditions with an initial MC concentration of 0.5 mM.

### **3.3 Sequential Reduction and Oxidation of Individual IMCs**

Batch reduction of DNAN, NTO, or NQ was carried out in an anaerobic glove box using 250-mL glass beakers containing 100 mL of MC solution and 0.12 g of nZVI for DNAN or 0.2 g of nZVI for NTO and NQ. The initial concentrations of DNAN, NTO, and NQ were 0.5, 2.5, and 2.5 mM, respectively. Solution pH was maintained at  $2.0 \pm 0.3$  through addition of 0.75 M  $H_2SO_4$  using a pH controller (Bluelab, New Zealand). An overhead digital mixer (Cole-Parmer, Vernon Hills, IL) was used to stir solution at 500 rpm for 10 min. The treated solution was then passed through a 0.22- $\mu$ m PTFE syringe filter to remove nZVI particles, and 50 mL of filtrate was used for a Fenton oxidation experiment. The remaining filtrate was used for quantification of MC reduction products, TOC, and TNb.

Fenton oxidation was initiated by adding 50 mL of  $H_2O_2$  solution to 50 mL of nZVI-treated MC solution. The initial concentrations of added  $H_2O_2$  were 13 mM for

DNAN and 22 mM for NTO and NQ. The H<sub>2</sub>O<sub>2</sub> concentrations were chosen based on the amount of Fe(II) generated from reduction experiments to give a Fe(II)-to-H<sub>2</sub>O<sub>2</sub> mole ratio of 1:2. Preliminary tests showed that a molar ratio of 1:2 appeared to be optimal and additional H<sub>2</sub>O<sub>2</sub> did not enhance TOC removal. Reaction mixture was placed on a stir plate at 150 rpm and allowed to react for 20 min, as preliminary tests showed that TOC removal beyond 20 min was negligible. Solution pH was maintained at 2.0±0.3 using a pH controller. Fifty mL of sample was collected and passed through a 0.22-µm PTFE syringe filter for analyses.

### **3.4 Sequential Reduction and Oxidation of Synthetic Wastewater**

Sequential reduction-oxidation experiments were conducted with a synthetic wastewater containing all three MCs (DNAN, NTO and NQ) to further evaluate the feasibility of the proposed process to degrade IM constituents. The initial concentrations were 0.5 mM for DNAN, 1.75 mM for NTO, and 3.5 mM for NQ. These concentrations were chosen to yield the same initial TOC of ca. 42 mg/L for each MC. Reduction experiments were carried out in 60-mL borosilicate amber reactors containing 40 mL of deoxygenated test solution, and reaction was initiated by addition of 200 mg of nZVI. Four mL of 0.75 M H<sub>2</sub>SO<sub>4</sub> was added to maintain the pH at 2.0 ± 0.3 during reduction. Reactors were placed on an end-over-end shaker for 10 min and solution was passed through a 0.22-µm PTFE syringe filter to remove residual nZVI. Filtrate was collected for chemical analyses and for an oxidation experiment.

Fenton oxidation was carried out in 60-mL glass reactors containing 20 mL of reduced wastewater and was initiated by addition of 10 mL of 0.12 M H<sub>2</sub>O<sub>2</sub> solution.

As the concentration of Fe(II) was determined to be 42 mM in the reduced wastewater under the test conditions, the amount of H<sub>2</sub>O<sub>2</sub> was chosen to yield an initial H<sub>2</sub>O<sub>2</sub> concentration of 84 mM (i.e., Fe(II)-to-H<sub>2</sub>O<sub>2</sub> = 1:2 by mole). Reactors were shaken at 150 rpm and the reaction time was 20 min for all experiments. All liquid samples were 0.22- $\mu$ m filtered before analysis.

### 3.5 Analytical Methods

DNAN, NTO, NQ, DAAN, ATO, and the two common DNAN reduction intermediates 2-amino-4-nitroanisole (2A4NAN) and 4-amino-2-nitroanisole (4A2NAN) were all quantified using an Agilent 1260 series high-performance liquid chromatograph (HPLC) equipped with diode-array detector (DAD). For NTO, ATO, and NQ analysis, the stationary phase was a Hypercarb<sup>TM</sup> porous graphitic carbon LC column (4.6 mm x 100 mm, particle size 5.0  $\mu$ m, Thermo Fisher Scientific, Waltham, MA), and the mobile phase was 0.1% aqueous TFA and acetonitrile at a flowrate of 2 mL/min. The injection volume was 75  $\mu$ L. NTO was detected at 8.2 min/318 nm, ATO at 4.2 min/210 nm, and NQ at 5.7 min/260 nm. For DNAN, 4A2NAN, 2A4NAN, and DAAN, the stationary phase was a Zorbax SB-C18 column (4.6 mm x 50 mm, particle size 3.5  $\mu$ m, Agilent, Santa Clara, CA). The mobile phase consisted of methanol and 50 mM sodium phosphate buffer, with a flowrate of 1.7 mL/min. The sample injection volume was 100  $\mu$ L. DNAN was detected at 4.8 min/214 nm, 4A2NAN at 3.2 min/234 nm, 2A4NAN at 4.2 min/254 nm, and DAAN at 2.3 min/210 nm. The retention times and wavelengths in all cases were chosen based on reference standards of MCs and their reduction products acquired from AccuStandard (New Haven, CT).

Nitrate and nitrite were measured using a Dionex ICS-1000 ion chromatograph (IC) (Dionex, Sunnyvale, CA) equipped with a Dionex AERS 500 suppressor, a Dionex IonPac AS23 capillary column preceded by a Dionex IonPac AG23 guard column. Separation was achieved at 30 °C using a mixture of 4.5 mM Na<sub>2</sub>CO<sub>3</sub> and 0.8 mM NaHCO<sub>3</sub> as eluent. Aqueous Fe(II) and total Fe were quantified with a UV-vis spectrophotometer (Vernier, Beaverton, OR) at 511 nm using the 1,10-phenanthroline method. Aqueous Fe(III) concentration was obtained based on the difference between aqueous Fe(II) and total Fe concentrations. Ammonia was measured with a Hach DR5000 UV-vis spectrophotometer (Loveland, CO). TOC and TNb concentrations were quantified using an Elementar Vario TOC Cube (Elementar Americas Inc., Ronkonkoma, NY) at the University of Delaware's Soil Testing Laboratory.

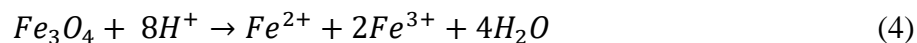
## Chapter 4

### RESULTS AND DISCUSSIONS

#### 4.1 IMC Reduction by nZVI

As shown in Figure 4.1, in synthetic wastewater at pH 2.0, NTO, DNAN, and NQ were reduced simultaneously by 30 mg of nZVI. Note that Figure 4.1 is a semi-log plot, and therefore the changing slopes indicate that these reactions were not pseudo-first-order with respect to MC concentration (Eq. 3) under the test conditions. That is,  $k_{obs}$  was not constant but decreased with time, presumably due to diminishing mass and surface area of nZVI as it was oxidized rapidly and continuously by the MCs, proton, or both.

$$\ln\left(\frac{[MC]}{[MC]_0}\right) = -k_{obs}t \quad (3)$$



The air-stable Nanofer STAR nZVI used in this work contained 65–80% Fe(0) and 20–35% magnetite (Fe<sub>3</sub>O<sub>4</sub>) by mass, as reported by the manufacturer. If all Fe(0) was oxidized to Fe(II) (Eq. 2) and all Fe<sub>3</sub>O<sub>4</sub> was acid-dissolved to Fe(II) and Fe(III) (at a mole ratio of 1:2; Eq. 4), then Fe(III) should account for between 10% and 19% (for 80% and 65% Fe(0) content, respectively) by mole of total dissolved Fe in the final solution. This was not observed. As shown in Figure A4, Fe(II) accounted for almost all the total dissolved Fe in all three nZVI-reduced MC solutions. This

indicates that, at pH 2.0, Fe(0) was oxidized almost completely to Fe(II) by MCs and/or proton, that Fe(II) could not reduce any of the MCs, and that most Fe(III) dissolved from Fe<sub>3</sub>O<sub>4</sub> was reduced by Fe(0) to Fe(II), as shown in Eq. (5). Reduction of Fe(III) would decrease the amount of electron in Fe(0) available for MC reduction, but was necessary to provide chemical stability to the nZVI. Taking into account Eq. (5), the amount of electron available in 30 mg of Nanofer STAR was 0.61–0.81 mmol, for 65% and 80% Fe(0) content, respectively.

As will be discussed below, the electron demands of DNAN and NTO are 6 e<sup>-</sup> per nitro group; i.e., each NTO molecule would accept 6 electrons and each DNAN molecule 12 electrons. If we assume the same electron demand holds for NQ (i.e., 6 e<sup>-</sup> per NQ molecule), then the total electron demand from the three MCs combined in the 40-mL solution would be 0.48 mmol, or 59–79% of the available electrons in 30 mg of nZVI. Although the MCs were not completely reduced in 30 min (Figure 4.1), the extents of reaction would have consumed approximately half of all the available electrons. Hence, the electron balance calculation shows that nZVI was not in large excess and the reaction conditions were not pseudo-first-order, which explains the decreasing rates of reduction over time for all three MCs. Note that anaerobic oxidation of Fe(0) by proton (Eq. 2) may or may not be a net electron sink. The nascent atomic hydrogen formed on the nZVI surface (H<sub>(ads)</sub>) may either react with MCs (Oh et al., 2002) or self-couple to produce H<sub>2</sub> (Eq. 6), and only the latter represents a loss mechanism (2 e<sup>-</sup> per H<sub>2</sub> molecule formed). Due to the 2% H<sub>2</sub> background in the glove box atmosphere, however, it was not possible to quantify H<sub>2</sub> production during MC reduction experiments.



Additional experiments were performed under similar conditions with increased nZVI mass in an attempt to obtain pseudo-first-order rate constants ( $k_{obs}$ ). However, the MC disappearance rates quickly became too fast to measure accurately: Over 95% of all three MCs were transformed within 10 min when nZVI mass was doubled (to 60 mg, Figure 4.2) and no MC could be detected when nZVI mass was doubled again (to 120 mg) (Figure 4.2). A control reactor without nZVI showed no degradation of MCs (Figure A2). Although it was not possible to obtain  $k_{obs}$  for the three MCs under the condition of this study, the data clearly show that, in contrast to the chemical and biological processes that have been investigated to date, (n)ZVI can simultaneously degrade all three MCs and, in particular, is the first chemical agent reported to rapidly degrade NQ.

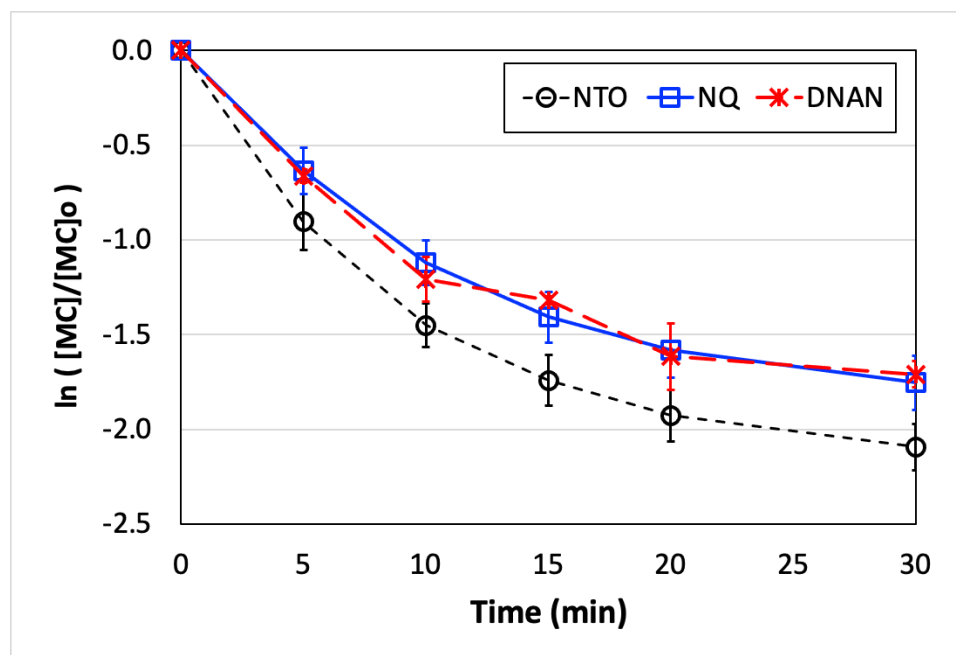


Figure 4.1 Concentrations of NTO, DNAN, and NQ during reduction by 30 mg of nZVI. All three MCs were in same reactor at an equal initial concentration of 0.5 mM. The solution volume was 40 mL. The pH was  $2.0 \pm 0.4$ . Error bars are based on duplicate reactors.

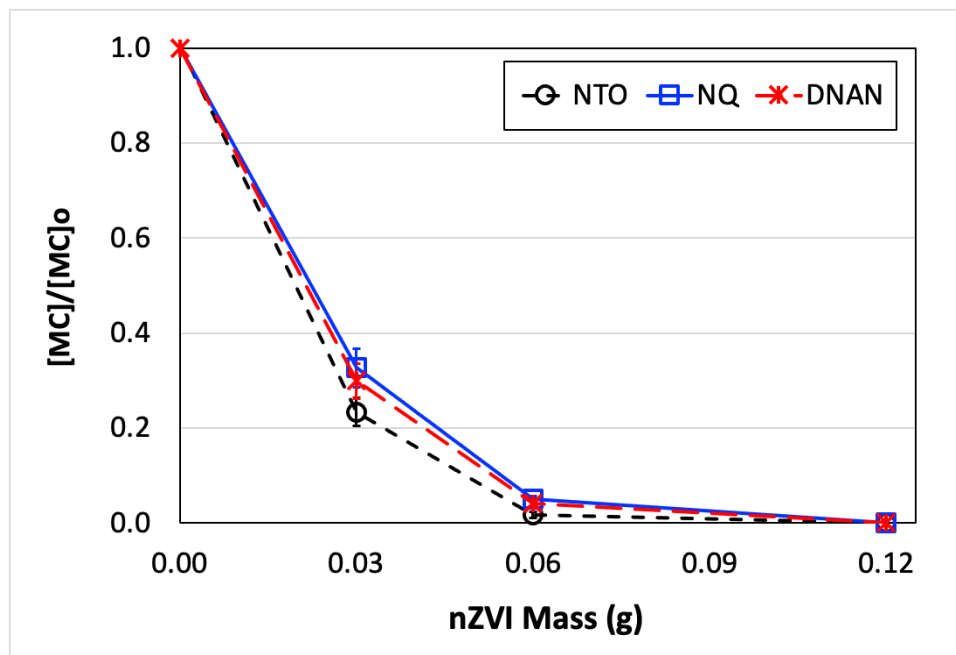


Figure 4.2 Concentrations of NTO, DNAN, and NQ 10 min after reduction by 30, 60, and 120 mg of nZVI. All three MCs were in same reactor at an equal initial concentration of 0.5 mM. The solution volume was 40 mL. The pH was  $2.0 \pm 0.4$ . Error bars are based on duplicate reactors.

Batch experiments were also performed with individual IMCs to identify and quantify their reduction products. Nitroaromatic compounds (NACs) have been shown to react with ZVI through reduction of the nitro group ( $-\text{NO}_2$ ) to amino group ( $-\text{NH}_2$ ), involving transfer of  $6 e^-$  and oxidation of 3 Fe(0) atoms per nitro group (Oh et al., 2002, 2005), as shown in Eq. (7). DNAN and NTO (more specifically, the singly deprotonated form of NTO) are both NACs and have been shown to undergo reductive transformation to DAAN through 2-amino-4-nitroanisole (2A4NAN) and 4-amino-2-

nitroanisole (4A2NAN) as intermediates and to ATO, respectively, by Fe(II) reductants including green rust and the hematite-Fe(II) redox pair (Hawari et al., 2015; Khatiwada et al., 2018; Cárdenas-Hernández et al., 2020). Therefore, these reduction products of DNAN and NTO were looked for first.

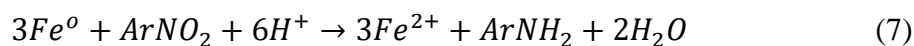


Figure 4.3 shows disappearance of NTO and formation of ATO following nZVI addition. NTO was removed completely in 20 min and >95% of the NTO transformed was recovered as ATO in 30 min. The mass balance gap (black circles) during the reaction, as well as the lag time between complete NTO removal and maximum ATO production, suggest an intermediate(s) was present in significant quantity during NTO reduction by nZVI. This intermediate may potentially be 3-nitroso-1,2,4-triazol-5-one and/or 3-hydroxyamino-1,2,4-triazol-5-one; i.e., the two- and four-electron reduction products of NTO, respectively. However, reference standards of these compounds were not commercially available for confirmation.

Figure 4.4 shows the disappearance of DNAN and concomitant formation of its reduction end product, DAAN. While both 4A2NAN and 2A4NAN were detected during DNAN reduction, their concentrations were negligible throughout the experiment. The lack of accumulation of these intermediates, and the high mass balance observed throughout the reaction, suggest that 4A2NAN and 2A4NAN were reduced instantly by nZVI as soon as they were formed. The final DAAN yield was 100%.

Similar to other NACs, NTO and DNAN were transformed by nZVI quantitatively to their reduction end products. The full mass and electron balances are

useful because they not only confirm the identity of the reduction products (DNAN and NTO), which would be the predominant compounds oxidized in the subsequent Fenton process, but also enable estimation of the electron demand of a given MC wastewater (i.e., 6 e<sup>-</sup> per NTO molecule and 12 e<sup>-</sup> per DNAN molecule) and the theoretical minimum nZVI mass required for complete reduction.

Similar attempts were made to identify aminoguanidine (AQ), a potential reduction product of NQ, through UV-vis, HPLC-DAD and LC-MS analyses. Although different LC columns, eluent compositions, gradients, and wavelengths were assessed using an AQ reference standard as well as clean NQ reduction solution, it was not possible to separate or detect AQ, presumably because of its highly polar nature and minimal LC retention. The experimental conditions under which the study was carried out rules out the possibility of sorption of NQ to Fe(III)-oxide surfaces as a mechanism for NQ disappearance observed. This is because Fe(III)-oxides will be thermodynamically unstable under such low pH ( $\approx 2$ ) reducing condition. Hence, although NQ was degraded by nZVI at a similar rate (Figure 4.5), mass and electron balances for NQ reduction were not established.

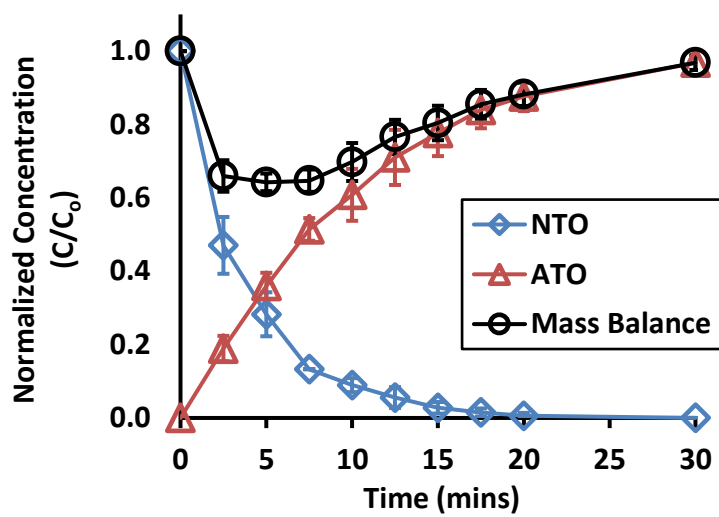


Figure 4.3 Disappearance of NTO and formation of its reduction product, following addition of 28.1 mg of Nanofer STAR. The initial concentration was 0.5 mM. Solution pH was constant at  $2.0 \pm 0.4$ . Error bars are based on duplicate reactors.

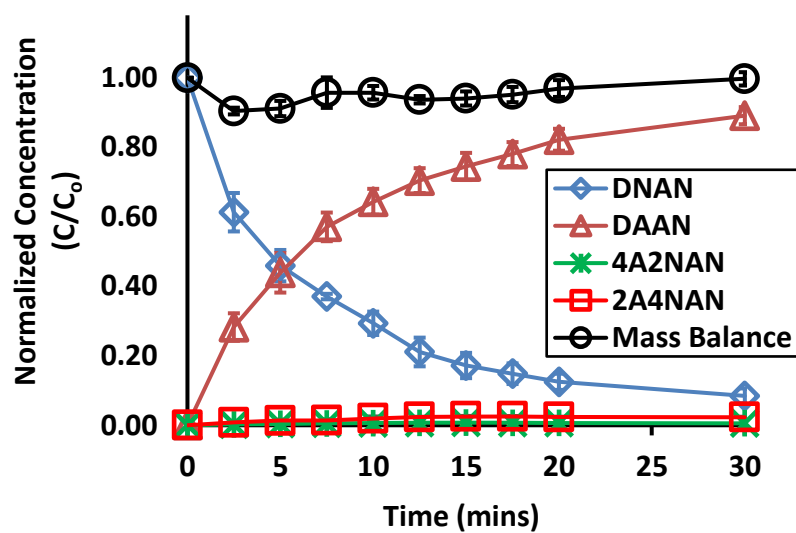


Figure 4.4 Disappearance of DNAN and formation of its reduction products, following addition of 28.1 mg of Nanofer STAR. The initial concentration was 0.5 mM. Solution pH was constant at  $2.0 \pm 0.4$ . Error bars are based on duplicate reactors.

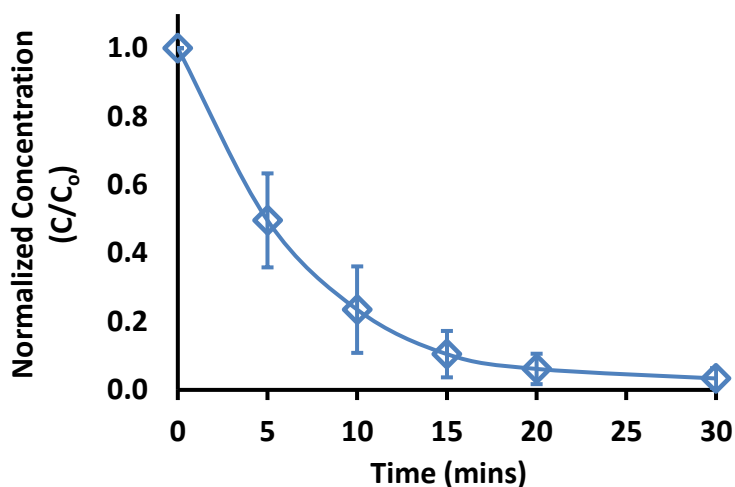


Figure 4.5 Disappearance of NQ following addition of 28.1 mg of Nanofer STAR. The reduction product(s) of NQ was not identified. The initial concentration was 0.5 mM. Solution pH was constant at  $2.0 \pm 0.4$ . Error bars are based on duplicate reactors.

## 4.2 TOC and Nitrogen Products

In addition to reduction intermediates and products, TOC, TNb, nitrate, and ammonia concentrations were measured before and after nZVI reduction and Fenton oxidation of individual MCs. As expected, reduction did not measurably change the TOC of MC solutions (Figure 4.6). This is consistent with the above result (Figure 4.3 and 4.4) that all the carbon atoms in NTO and DNAN, and presumably in NQ as well remained intact after reduction (Figure 4.6). Fenton oxidation of nZVI-treated NTO and DNAN solutions for 20 min resulted in 66% and 63% TOC removal, respectively

(Figure 4.6). Since both carbon atoms in ATO and six of the seven carbon atoms in DAAN are ring carbons, the TOC removal results show that both ATO and DAAN had been fragmented through ring cleavage during Fenton oxidation. HPLC analyses confirmed that both ATO and DAAN were absent after oxidation. In contrast, TOC removal for nZVI-reduced NQ solution was negligible: The TOC of NQ solution remained practically the same as that of control. Hence, the carbon atom in the NQ reduction product(s) – might it be AQ or other compounds – was more resistant to hydroxyl radical attack than those in ATO and DAAN. This might be related to the structure and high N/C mole ratio of NQ and AQ (Figure A1): with an N/C ratio of 4, the only carbon atom in NQ or AQ was well-protected by reduced nitrogen atoms, which would have to be oxidized by Fenton reagent before TOC mineralization could occur.

Figure 4.7 shows the TNb, NH<sub>3</sub>-N, and NO<sub>3</sub>-N concentrations for each MC. Because all samples were filtered (to remove nZVI particles) and because TNb captures only non-volatile N species, the fact that the total nitrogen mass stayed roughly constant before and after reduction and oxidation for all three MCs suggests that gaseous products (e.g., N<sub>2</sub>, N<sub>2</sub>O and NO) were not formed or only negligibly. Consistent with the high recoveries of ATO and DAAN, ammonia was not produced following NTO and DNAN reduction but accounted for a small fraction (ca. 8%) of the nitrogen in NQ reduction products. After oxidation, roughly 50% of the DNAN-N was recovered as NH<sub>3</sub>-N (46%) and NO<sub>3</sub>-N (3.5%), 30% of the NTO-N was recovered as NH<sub>3</sub>-N (24%) and NO<sub>3</sub>-N (6%), and only 14% of the NQ-N was recovered as NH<sub>3</sub>-N (9%) and NO<sub>3</sub>-N (5%) (Figure 4.7). While the yields were not high, formation of ammonia and nitrate following Fenton oxidation suggests that ATO, DAAN, and NQ

reduction products were all fragmented by hydroxyl radical. Nitrite was looked for but never detected in either reduction or oxidation samples for any of the MCs.

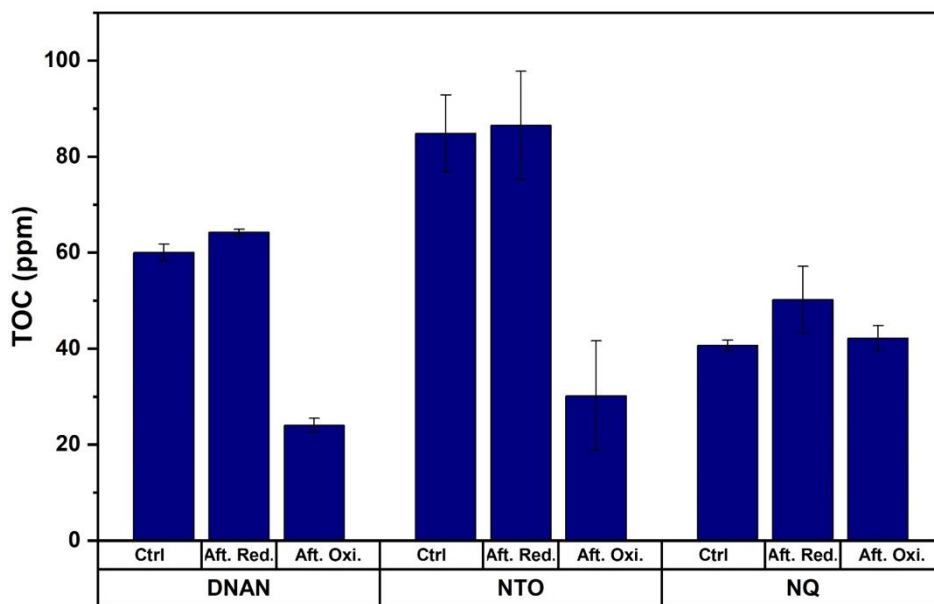


Figure 4.6 Concentrations of TOC in solutions containing individual MCs before reduction (Ctrl), after reduction (Aft. Red), and after oxidation (Aft. Oxi.). Reaction times were 10 min for reduction and 20 min for oxidation. pH was  $2.0 \pm 0.3$  for all solutions. Error bars are based on duplicate reactors.

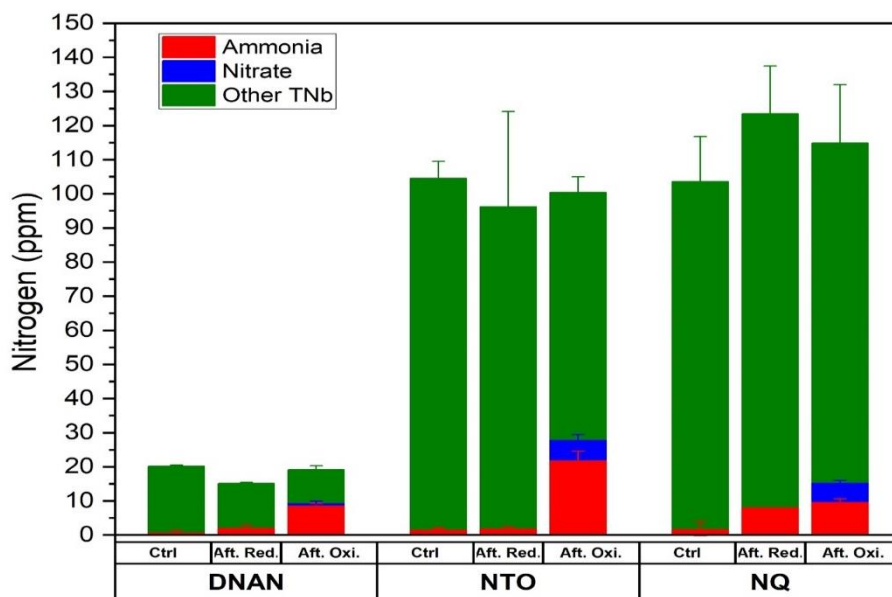


Figure 4.7 Concentrations of TNb in solutions containing individual MCs before reduction (Ctrl), after reduction (Aft. Red), and after oxidation (Aft. Oxi.). Reaction times were 10 min for reduction and 20 min for oxidation. pH was  $2.0 \pm 0.3$  for all solutions. Error bars are based on duplicate reactors.

### 4.3 Sequential Reduction and Oxidation of Synthetic Wastewater

To further evaluate the nZVI-H<sub>2</sub>O<sub>2</sub> process for MC wastewater treatment, a synthetic wastewater containing DNAN, NTO, and NQ at the same organic carbon concentration (3.5 mM or 42 mg/L each) was used for a sequential reduction-oxidation study. Complete reduction of all three MCs in 40 mL of wastewater was achieved within 10 min of reaction with 0.2 g of added nZVI. NTO and DNAN were recovered

as ATO and DAAN (96% and 80%, respectively) after reduction, and both products were completely degraded by Fenton oxidation (Figure A5). Similar to the results in Figures 4.6 and 4.7, the TOC and TNb of the synthetic wastewater was statistically unchanged before and after reduction (Figures 4.8 and 4.9), and a small amount (<10%) of NH<sub>3</sub>-N was detected which was presumably derived from NQ reduction (Figure 4.7). Oxidation of the nZVI-reduced MC wastewater resulted in 41% TOC removal (Figure 4.8), which closely matches the extent of mineralization (43%) estimated based on the values for reduced DNAN and NTO (63% and 66%, respectively) in Figure 4.6. Also consistent with the data in Figure 4.7, NH<sub>3</sub>-N (21%) and NO<sub>3</sub>-N (6%) combined accounted for ca. 27% of the TNb after Fenton oxidation (Figure 4.9). Ammonia was produced through oxidation of the reduction products of all three MCs, whereas nitrate was formed from oxidation of ATO and NQ reduction products (Figures 4.9 and 4.7). Again, nitrite was never detected.

Fenton oxidation of the three MCs were tested to determine whether Fenton reagents can degrade the parent IMCs. As shown in Figure A3, NTO and DNAN were degraded fully within 20 min, whereas NQ was degraded only to a limited extent. This result suggests that nZVI reduction would be a necessary pretreatment to fully degrade IMCs in munitions production wastewaters containing NQ.

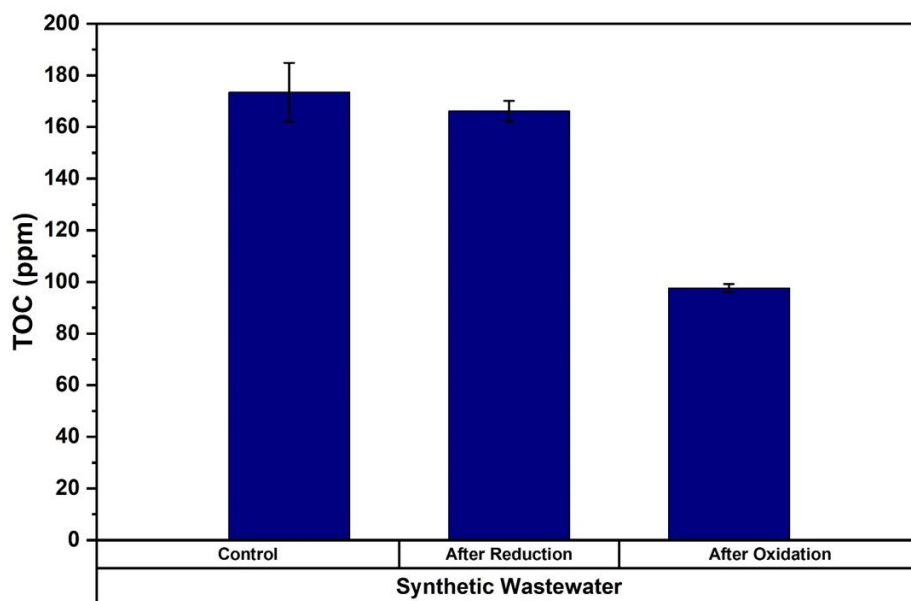


Figure 4.8 Concentrations of TOC in synthetic wastewater containing DNAN, NTO and NQ before reduction (Control), after reduction, and after oxidation. Reaction times were 10 min for reduction and 20 min for oxidation. pH was constant at  $2.0 \pm 0.3$ . Error bars are based on duplicate reactors.

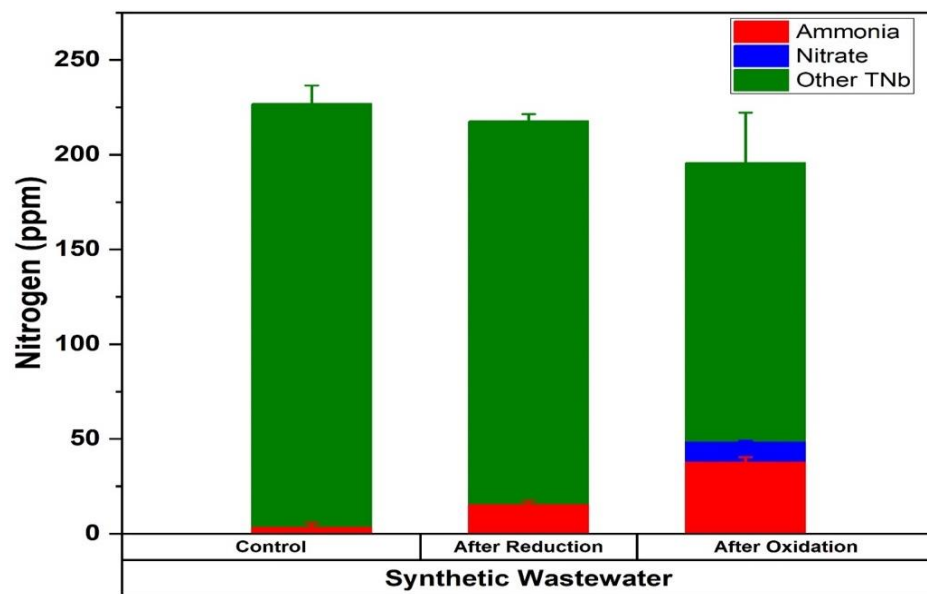


Figure 4.9 Concentrations of TNb in synthetic wastewater containing DNAN, NTO and NQ before reduction (Control), after reduction, and after oxidation. Reaction times were 10 min for reduction and 20 min for oxidation. pH was constant at  $2.0 \pm 0.3$ . Error bars are based on duplicate reactors.

## **Chapter 5**

### **PILOT SCALE STUDY**

#### **5.1 Relevance**

In an effort to evaluate the feasibility of the nZVI-H<sub>2</sub>O<sub>2</sub> technology for use at military facilities, a set of pilot study tests were carried out at a larger scale and volume. The pilot study was a scale-up from the small laboratory studies in chapters 3 and 4, by a factor of 50; and was only 15 times smaller than anticipated reactor sizes at military facilities. With this study, it was possible to determine whether it will be feasible to apply the nZVI-H<sub>2</sub>O<sub>2</sub> technology at military facilities.

#### **5.2 Pilot Scale Study: Methodology**

In these tests, a 2-gallon glass reactor was used to treat 5 liters of synthetic wastewater containing a single MC (NTO, DNAN or NQ). The solution was stirred by an electric overhead mixer (H. Hukoer Products, China) at 1200 rpm. Two stainless steel air stones were arranged in parallel and connected to a central nitrogen gas line for deoxygenation before and throughout each experiment. The nitrogen flow was maintained at 2 L/min. The tests were run at pH 2.0, to mirror the low pH of insensitive MC wastewaters. An automatic pH Controller (Bluelab, New Zealand) was used to dose concentrated H<sub>2</sub>SO<sub>4</sub> intermittently. See Figure 5.1 for schematic representation of the experimental set-up. The reduction step was initiated by adding nZVI in excess (stoichiometric) amount to the reactor. Aqueous samples were withdrawn from the bulk liquid through a built-in sampling line before and at different times after addition of nZVI. After reduction by nZVI, oxidation was initiated by H<sub>2</sub>O<sub>2</sub>

addition (at a Fe(II)-to-H<sub>2</sub>O<sub>2</sub> mole ratio of 1:2). Analyses for MCs and their reduction product(s) were carried out using the HPLC-DAD and conditions mentioned in Chapter 3; while TOC concentrations were determined using a TOC Analyzer (Shimadzu, OR). nZVI dosing and H<sub>2</sub>O<sub>2</sub> addition were at concentrations similar to those used in the small-scale experiments in chapters 3 and 4.

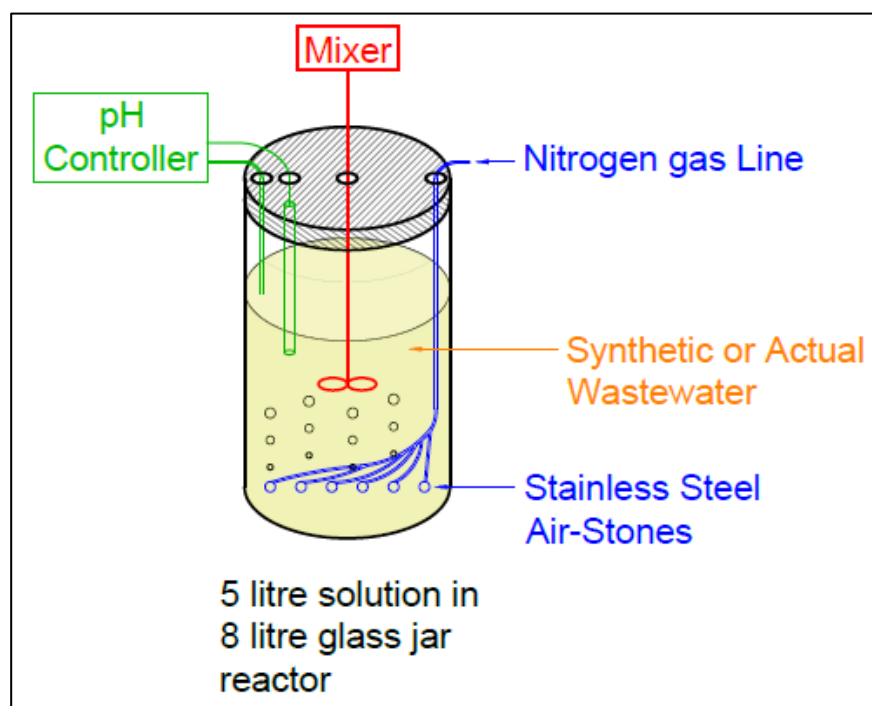


Figure 5.1 Schematic of Set-up for Pilot Scale Study Experiments

### 5.3 Pilot Scale Study: Results

The pilot scale experiments with single MCs (NTO, DNAN and NQ) showed rapid and complete degradation of all three parent MCs by nZVI in the reduction step.

All three MCs were degraded within 10 mins by nZVI (Figures 5.2 – 5.4). This is consistent with the findings from the small-scale experiments where rapid and complete degradation of parent IMCs by nZVI in 100 mL reactors was observed. NTO and DNAN reduction products were recovered as in the small-scale experiments. For NTO, 97% of its mass was recovered as ATO, while DNAN was recovered as DAAN, with 99% yield (Figures 5.2 and 5.3). Fenton oxidation, following reduction, yielded TOC removal in NTO and DNAN reduced solution. TOC removal was 60% and 34% in NTO and DNAN reduced solutions, respectively (Figure 5.5). Again, NQ reduced solution showed no TOC removal after oxidation (Figure 5.5).

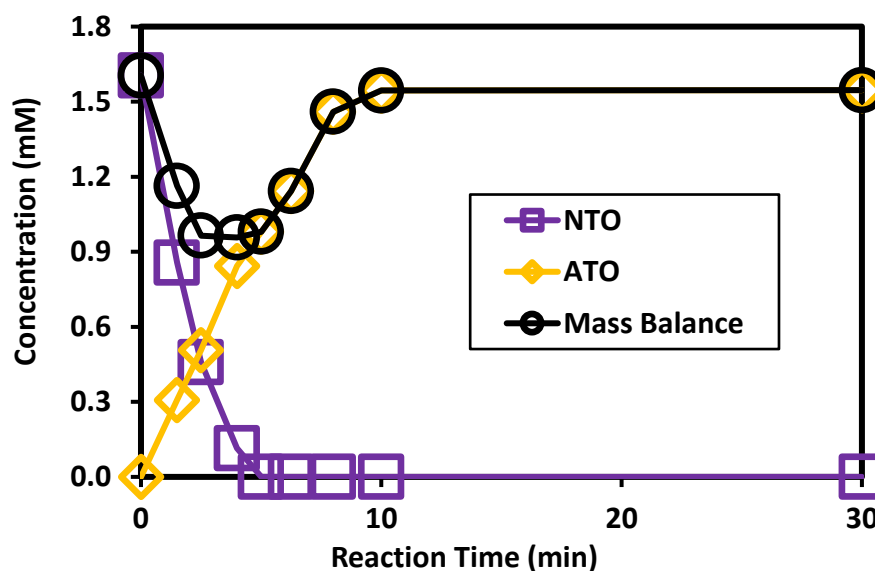


Figure 5.2 Disappearance of NTO and formation of its reduction product, ATO, with 2.0 g/L of Nanofer STAR at Pilot Scale. The initial concentration was 1.60 mM. Solution pH was constant at  $2.0 \pm 0.1$ .

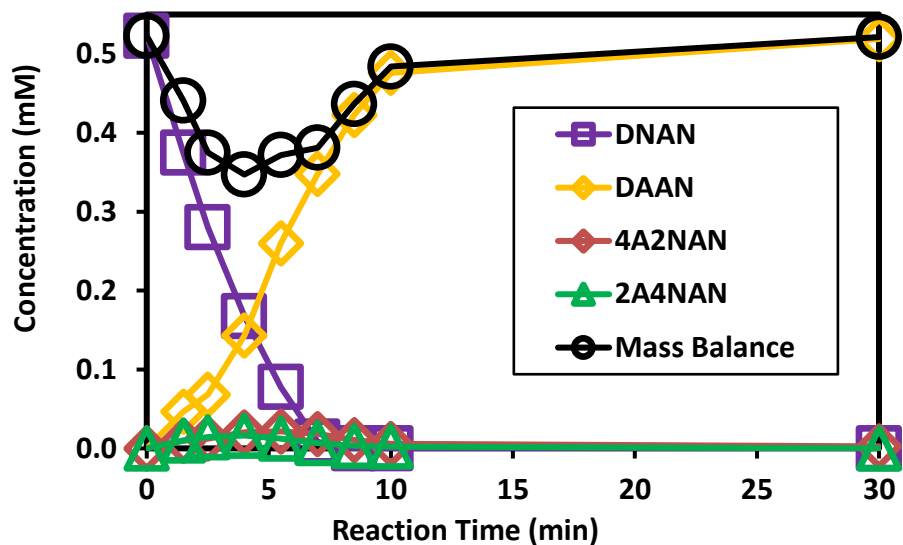


Figure 5.3 Disappearance of DNAN and formation of its reduction products, with 1.2 g/L of Nanofer STAR at Pilot Scale. The initial DNAN concentration was 0.5 mM. Solution pH was constant at  $2.0 \pm 0.1$ .

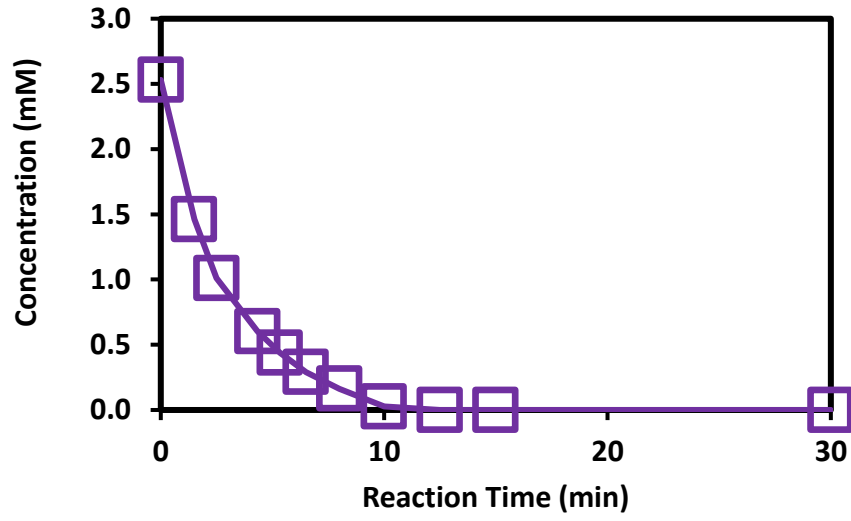


Figure 5.4 Disappearance of NQ, with 2.0 g/L of Nanofer STAR at Pilot Scale. The initial NQ concentration was 2.5 mM. Solution pH was constant at  $2.0 \pm 0.2$ .

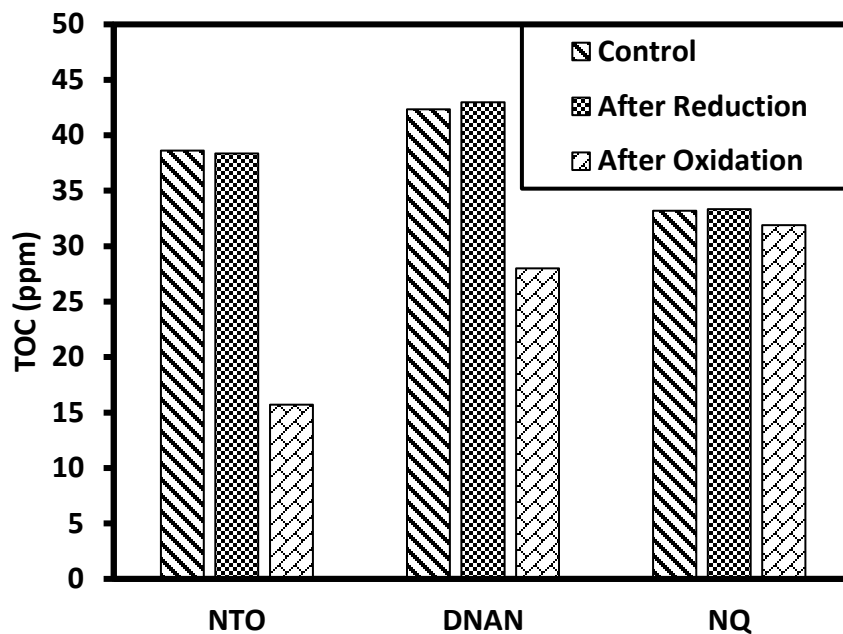


Figure 5.5 Concentrations of TOC in solutions containing individual MCs with Experiments at Pilot Scale before reduction (Control), after reduction (After Reduction), and after oxidation (After Oxidation). Reaction times were 30 min for reduction and 20 min for oxidation. pH was  $2.4 \pm 0.1$  for all solutions.

## Chapter 6

### CONCLUSION AND FUTURE RESEARCH

In this study, it was demonstrated that sequential nZVI-H<sub>2</sub>O<sub>2</sub> treatment process can rapidly and fully degrade three insensitive MCs that are major constituents in IMX formulations and production wastewaters. Mass and electron balances for NTO and DNAN reduction by nZVI were established. Results obtained with individual IMCs and with a synthetic wastewater are consistent with respect to transformation rate, extent of mineralization, and nitrogen product distribution. Hence, it may be possible to predict the treatment performance of the nZVI-H<sub>2</sub>O<sub>2</sub> process based on wastewater MC composition. This is the first report of NTO reduction by nZVI, and the first report of rapid NQ degradation by any abiotic or biological agent. The ability of nZVI to rapidly and simultaneously degrade all three MCs (as well as RDX (Oh et al., 2005), a constituent in IMX-104) makes nZVI an attractive candidate for munitions wastewater treatment. The results from the pilot study tests further validate the ability of nZVI-H<sub>2</sub>O<sub>2</sub> technology to degrade MCs rapidly and completely on a large scale and volume. The data heightens the feasibility of using this technology at military facilities where large volumes of IMX wastewaters (hundreds of gallons) will need to be treated, regularly.

Future work should focus on identifying NQ reduction product(s) and establishing mass and electron balances. In addition, as mineralization of MC reduction products was incomplete and a significant portion of the bound nitrogen species was unknown, it would be necessary to evaluate the toxicity and biodegradability of both MC reduction products and their Fenton oxidation products.

Lastly, key process parameters such as pH, mixing rate, nZVI dosing, etc, should be assessed to optimize the technology.

## REFERENCES

- Ahn, S. C.; Hubbard, B.; Cha, D. K.; Kim, B. J. Simultaneous Removal of Perchlorate and Energetic Compounds in Munitions Wastewater by Zero-Valent Iron and Perchlorate-Respiring Bacteria. *J. Environ. Sci. Health A*. 2014, 49, 575–583.
- Bae, S.; Hanna, K. Reactivity of Nanoscale Zero-Valent Iron in Unbuffered Systems: Effect of pH and Fe(II) Dissolution. *Environ. Sci. Technol.* 2015, 49, 17, 10536–10543.
- Cárdenas-Hernández, P. A.; Anderson, K. A.; Murillo-Gelvez, J.; Di Toro, D. M.; Allen, H. E.; Carbonaro, R. F.; Chiu, P. C. Reduction of 3-Nitro-1,2,4-Triazol-5-One (NTO) by the Hematite–Aqueous Fe(II) Redox Couple. *Environ. Sci. Technol.*, 2020, 54, 12191–12201.
- Cheng, I. F.; Muftikian, R.; Fernando, Q.; Korte, N. Reduction of Nitrate to Ammonia by Zero-Valent Iron. *Chemosphere* 1997, 35, 2689-2695.
- Cheng, J. IMX 101/104 development into new and legacy weapon systems: environmental, safety, and occupational health (ESOH) concerns and project manager (PM) perspective. Johnson, M. S. (ed) JANNAF Workshop Proceedings - Fate, Transport and Effects of Insensitive Munitions: Issues and Recent Data. 2014, 7-11.
- Crouse, L. C.; Lent, E. M.; Leach, G. J. Oral Toxicity of 3-Nitro-1,2,4-triazol-5-one in Rats. *Int. J. Toxicol.* 2015, 34, 55-66.
- Chew, S. C.; Tennant, M.; Mai, N.; McAteer, D.; Pons, J. Practical Remediation of 3-nitro-1,2,4-triazol-5-one Wastewater. *Propell. Explos. Pyrot.* 2018, 43, 198–202.
- Dave, G.; Nilsson, E.; Wernersson, A. Sediment and Water Phase Toxicity And UV-activation of Six Chemicals used in Military Explosives. *Aquat. Ecosyst. Health* 2000, 3, 291-299.

- Davies, P. J.; Provas, A. Characterization of 2,4-Dinitroanisole: An Ingredient for Use in Low Sensitivity Melt Cast Formulations, Australian Government Department on Defence, Defence Science and Technology Organization Technical Report, DSTO-TR-1904. 2006.
- Devlin, J. F.; Klausen, J.; Schwarzenbach, R. P. Kinetics of Nitroaromatic Reduction on Granular Iron in Recirculating Batch Experiments. *Environ. Sci. Technol.* 1998, 32, 1941–1947.
- Felt, D.; Johnson, J.; Larson, S.; Hubbard, B.; Henry, K.; Nestler, C.; Ballard, J. Evaluation of Treatment Technologies for Wastewater from Insensitive Munitions Production. *Phase 1: Technology Down-Selection. Engineer Research and Development Center, ERDC/EL TR-13-20* November 2013, Vicksburg, MS.
- Fida, T. T.; Palamuru, S.; Pandey, G.; Spain, J. C. Aerobic Biodegradation of 2,4-Dinitroanisole by *Nocardioides* sp. Strain JS1661. *Appl. Environ. Microbiol.* 2014, 80, 7725-7731.
- Gent, D. B.; Thompson, A.; Waisner, S. A.; Johnson, J. L.; Smolinski, B.; O'Connor, G. The Evaluation of Treatment Technologies for Process Wastewater Resulting from IMX-101 Production. *U.S. Army Engineer Research and Development Center, ERDC/EL TR-13-16* 2013, Vicksburg, MS.
- Hawari, J.; Monteil-Rivera, F.; Perreault, N. N.; Halasz, A.; Paquet, L.; Radovic-Hrapovic, Z.; Deschamps, S.; Thiboutot, S.; Ampleman, G. Environmental Fate of 2,4-dinitroanisole (DNAN) and its Reduced Products. *Chemosphere* 2015, 119, 16–23.
- Huang, C. P.; Dong, C.; Tang, Z. Advanced Chemical Oxidation: Its Present Role and Potential Future in Hazardous Waste Treatment. *Waste Manage.* 1993, 13, 361-377.
- Indest, K. J.; Hancock, D. E.; Crocker, F. H.; Eberly, J. O.; Jung, C. M.; Blakeney, G. A.; Brame, J.; Chappell, M. A. Biodegradation of Insensitive Munition Formulations IMX101 and IMX104 in Surface Soils. *J. Ind. Microbiol. Biotechnol.* 2017, 44, 987-995.
- Isler, J. The Transition to Insensitive Munitions (IM). *Propell. Explo. Pyrot.* 1998, 23, 283-291.

- Jiang, Z.; Lv, L.; Zhang, W.; Du, Q.; Pan, B.; Yang, L.; Zhang, Q. Nitrate Reduction using Nanosized Zero-Valent Iron Supported by Polystyrene Resins: Role of Surface Functional Groups. *Water Res.* 2011, 45, 2191-2198.
- Johnson, M. S., Eck, W. S., Lent, E. M. Toxicity of Insensitive Munition (IMX) Formulations and Components. *Propell. Explo. Pyrot.* 2017, 42, 9-16.
- Kanel, S. R.; Manning, B.; Charlet, L.; Choi, H. Removal of Arsenic(III) from Groundwater by Nanoscale Zero-Valent Iron. *Environ. Sci. Technol.* 2005, 39, 1291-1298.
- Kaplan, D. L.; Cornell, J. H.; Kaplan, A. M. Decomposition of Nitroguanidine. *Environ. Sci. Technol.* 1982, 16, 488-492.
- Keum, Y.; Li, Q. X. Reduction of Nitroaromatic Pesticides with Zero-Valent Iron. *Chemosphere* 2004, 54, 255-263.
- Khatiwada, R.; Root, R. A.; Abrell, L.; Sierra-Alvarez, R.; Field, J. A.; Chorover, J. Abiotic Reduction of Insensitive Munition Compounds by Sulfate Green Rust. *Environ. Chem.* 2018, 15, 259–266.
- Kim, Y.; Carraway, E. R. Dechlorination of Pentachlorophenol by Zero Valent Iron and Modified Zero Valent Irons. *Environ. Sci. & Technol.* 2000, 34, 2014-2017.
- Kim, I.; Akanbi, O. E.; Cha, D. K.; Chiu, P. C.; Attavane, A. A.; Hubbard, B. P. Field Demonstration of an Integrated Nanoscale Zero Valent Iron-Hydrogen Peroxide Process for Complete Destruction of Munitions Compounds in Wastewater. Poster presented at: *Annual SERDP-ESTCP Technical Symposium and Workshop*, 2019. Washington, DC.
- Krzmarzick, M. J.; Khatiwada, R.; Olivares, C. I.; Abrell, L.; Sierra-Alvarez, R.; Chorover, J.; Field, J. A. Biotransformation and Degradation of the Insensitive Munitions Compound, 3 Nitro-1,2,4-triazol-5-one, by Soil Bacterial Communities. *Environ. Sci. Technol.* 2015, 49, 5681-5688.
- Lin, K.; Dehvari, K.; Hsien, M.; Hsu, P.; Kuo, H. Degradation of TNT, RDX, and HMX Explosive Wastewaters Using Zero-Valent Iron Nanoparticles. *Propellants, Explosives, Pyrotechnics* 2013, 38, 786-790.

- Lotufo, G. R.; Stanley, J. K.; Chappell, P.; Melby, N. L.; Wilbanks, M. S.; Gust, K. A. Subchronic, Chronic, Lethal and Sublethal Toxicity of Insensitive Munitions Mixture Formulations Relative to Individual Constituents in *Hyalella Azteca*. *Chemosphere* 2018, 210, 795-804.
- Lowry, G. V.; Johnson, K. M. Congener-Specific Dechlorination of Dissolved PCBs by Microscale and Nanoscale Zerovalent Iron in a Water/Methanol Solution. *Environ. Sci. Technol.* 2004, 38, 5208-5216.
- Madeira, C. L.; Speet, S. A.; Nieto, C. A.; Abrell, L.; Chorover, J.; Sierra-Alvarez, R.; Field, J. A. Sequential Anaerobic-Aerobic Biodegradation of Emerging Insensitive Munitions Compound 3-nitro-1,2,4-triazol-5-one (NTO). *Chemosphere* 2017, 167, 478-484.
- Madeira, C. L.; Field, J. A.; Simonich, M. T.; Tanguay, R. L.; Chorover, J.; Sierra-Alvarez, R. Ecotoxicity of the Insensitive Munitions Compound 3-nitro-1,2,4-triazol-5-one (NTO) and its Reduced Metabolite 3-amino-1,2,4-triazol-5-one (ATO). *J. Hazard. Mater.* 2018, 343, 340-346.
- Madeira, C. L.; Jog, K. V.; Vanover, E. T.; Brooks, M. D.; Taylor, D. K.; Sierra-Alvarez, R.; Waidner, L. A.; Spain, J. C.; Krzmarzick, M. J.; Field, J. A. Microbial Enrichment Culture Responsible for the Complete Oxidative Biodegradation of 3-amino-1,2,4-triazol-5-one (ATO), the Reduced Daughter Product of the Insensitive Munitions Compound 3-Nitro-1,2,4-triazol-5-one (NTO). *Environ. Sci. Technol.* 2019, 53, 12648-12656.
- Matheson, L. J.; Tratnyek, P. G. Reductive Dehalogenation of Chlorinated Methane by Iron Metal. *Environ. Sci. Technol.* 1994, 28, 2045-2053.
- Mu, Y.; Yu, H.; Zheng, J.; Zhang, S.; Sheng, G. Reductive Degradation of Nitrobenzene in Aqueous Solution by Zero-Valent Iron. *Chemosphere* 2004, 54, 789-794.
- Oh, S. Y.; Cha, D. K.; Kim, B. J.; Chiu, P. C. Effect of Adsorption to Elemental Iron on the Transformation of 2,4,6-trinitrotoluene and Hexahydro-1,3,5-trinitro-1,3,5-triazine in Solution. *Environ. Toxicol. Chem.* 2002, 21, 1384-1389.
- Oh, S. Y.; Cha, D. K.; Kim, B. J.; Chiu, P. C. Reduction of Nitroglycerin with Elemental Iron: Pathway, Kinetics, and Mechanisms. *Environ. Sci. Technol.* 2004, 38, 3723-3730.

- Oh, S. Y.; Cha, D. K.; Kim, B. J.; Chiu, P. C. Transformation of Hexahydro-1,3,5-trinitro-1,3,5-triazine (RDX), Octahydro-1,3,5,7-tetranitro-1,3,5,7-tetrazocine (HMX), and Methylene-dinitramine (MDNA) with Elemental Iron. *Environ. Toxicol. Chem.* 2005, 24, 2812–2819.
- Oh, S. Y.; Chiu, P. C.; Kim, B. J.; Cha, D. K. Enhancing Fenton Oxidation of TNT and RDX through Pretreatment with Zerovalent Iron. *Water Res.* 2003, 37, 4275–4283.
- Olivares, C. I.; Abrell, L.; Khatiwada, R.; Chorover, J.; Sierra-Alvarez, R.; Field, J. A. (Bio)transformation of 2,4-dinitroanisole (DNAN) in Soils. *J. Hazard. Mater.* 2016, 304, 214-221.
- Platten, W. E.; Bailey, D.; Suidan, M. T.; Maloney, S. W. Biological Transformation pathways of 2,4-dinitroanisole and N-methyl-para-nitroaniline in Anaerobic Fluidized-bed Bioreactors. *Chemosphere* 2010, 81, 1131-1136.
- Perey, J. R.; Chiu, P. C.; Huang, C. P.; Cha, D. K. Zero-Valent Iron Pretreatment for Enhancing the Biodegradability of Azo Dyes. *Water Environ. Res.* 2002, 74, 221–225.
- Perreault, N. N.; Halasz, A.; Manno, D.; Thiboutot, S.; Ampleman, G.; Hawari, J. Aerobic Mineralization of Nitroguanidine by Variovorax Strain VC1 Isolated from Soil. *Environ. Sci. Technol.* 2012, 46, 6035-6040.
- Richard, T.; Weidhaas, J. Biodegradation of IMX-101 explosive formulation constituents: 2,4-Dinitroanisole (DNAN), 3-nitro-1,2,4-triazol-5-one (NTO), and nitroguanidine. *J. Hazard. Mater.* 2014, 280, 372-379.
- Roberts, A. L.; Totten, L. A.; Arnold, W. A.; Burris, D. R.; Campbell, T. J. Reductive Elimination of Chlorinated Ethylenes by Zero-Valent Metals. *Environ. Sci. Technol.* 1996, 30, 2654-2659.
- Singh, J.; Comfort, S. D.; Shea, P. J. Remediating RDX Contaminated Water and Soil using Zero-Valent Iron. *J. Environ. Qual.* 1998, 27, 1240–1245.
- Sokkalingam, N.; Potoff, J.J.; Boddu, V.M.; Maloney, S.W. Prediction of Environmental Impact of High-Energy Materials with Atomistic Computer Simulations. ADM002187. *Army Science Conference (26th)* Orlando, FL, December 2008.

- Spear, R. J.; Louey, C. N.; Wolfson, M. G. A Preliminary Assessment of NTO as an Insensitive High Explosive. Australian Government Department on Defence, Defence Science and Technology Organization (DSTO) Materials Research Laboratory (MRL) Technical Report MRL-RT-89-18.1989.
- Terracciano, A.; Christodoulatos, C.; Koutsospyros, A.; Zheng, Z.; Su, T. L.; Smolinski, B.; Arienti, P.; Meng, X. Degradation of 3-Nitro-1,2,4-Trizole-5-One (NTO) in Wastewater with UV/H<sub>2</sub>O<sub>2</sub> Oxidation. *Chem. Eng. J.* 2018, 354, 481– 491.
- Xu, J.; Wang, Y.; Weng, C.; Bai, W.; Jiao, Y.; Kaegi, R.; Lowry, G. V. Reactivity, Selectivity, and Long-Term Performance of Sulfidized Nanoscale Zerovalent Iron with Different Properties. *Environ. Sci. Technol.* 2019, 53, 5936-5945.
- Ye, J.; Chiu, P. C. Transport of Atomic Hydrogen through Graphite and Its Reaction with Azoaromatic Compounds. *Environ. Sci. Technol.* 2006, 40, 3959-3964.

## Appendix

### SUPPLEMENTARY FIGURES

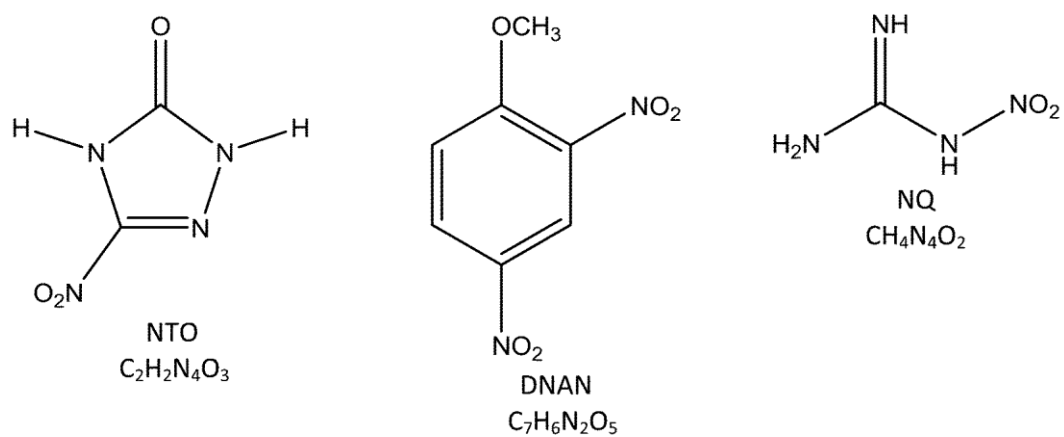


Figure A1 Structures of the insensitive munitions compounds- NTO, DNAN, and NQ. The molecular masses of NTO, DNAN, and NQ are 130.06, 198.13, and 104.07 g/mol, respectively.

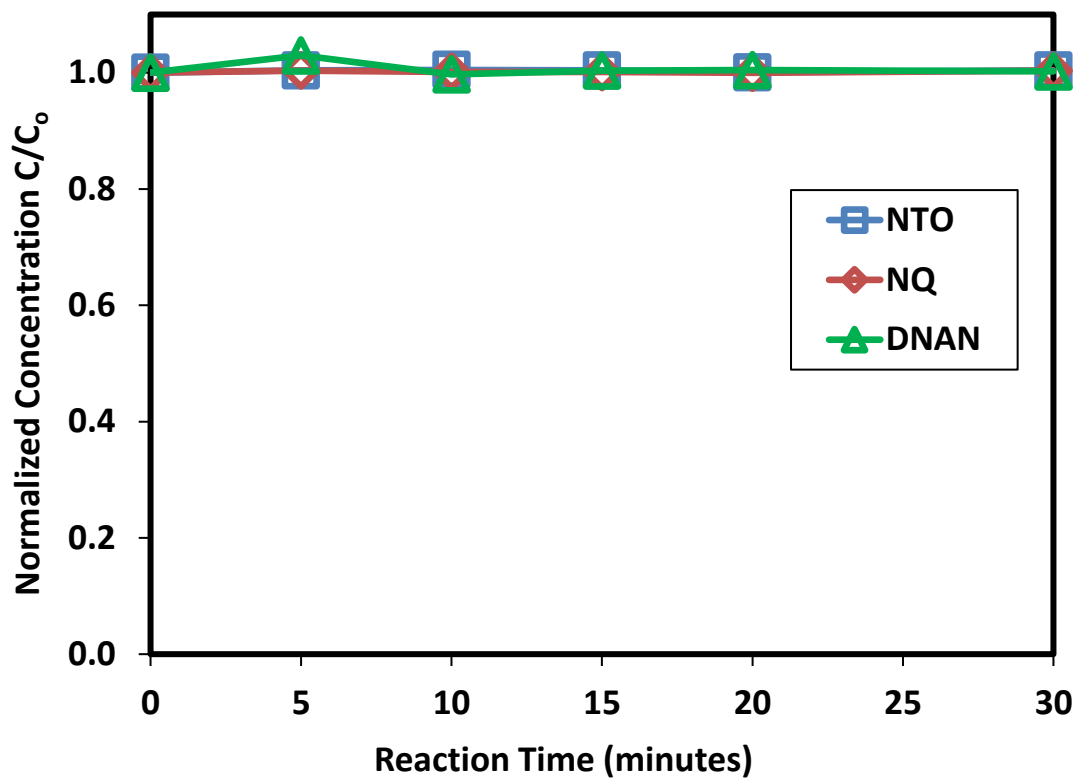


Figure A2 Control (no nZVI) for reduction experiments. Solution volume was 40 mL, pH was  $2.0 \pm 0.4$ , and initial concentration of each MC was 0.5 mM.

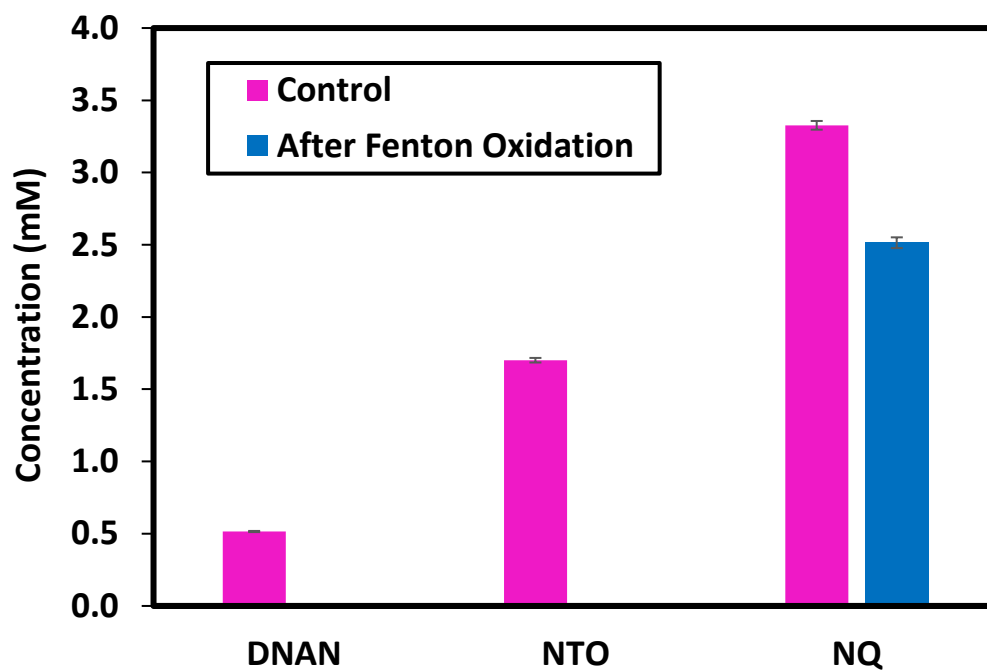


Figure A3 Concentrations of MCs in synthetic wastewater before (control, magenta) and after (blue) Fenton oxidation. Solution volume was 30 mL.  $\text{FeSO}_4$  and  $\text{H}_2\text{O}_2$  were added to give initial aqueous  $\text{Fe(II)}$  and  $\text{H}_2\text{O}_2$  concentrations of 42 mM and 84 mM, respectively. Reaction time was 20 min and pH was  $2.0 \pm 0.4$ . Error bars are based on duplicate reactors.

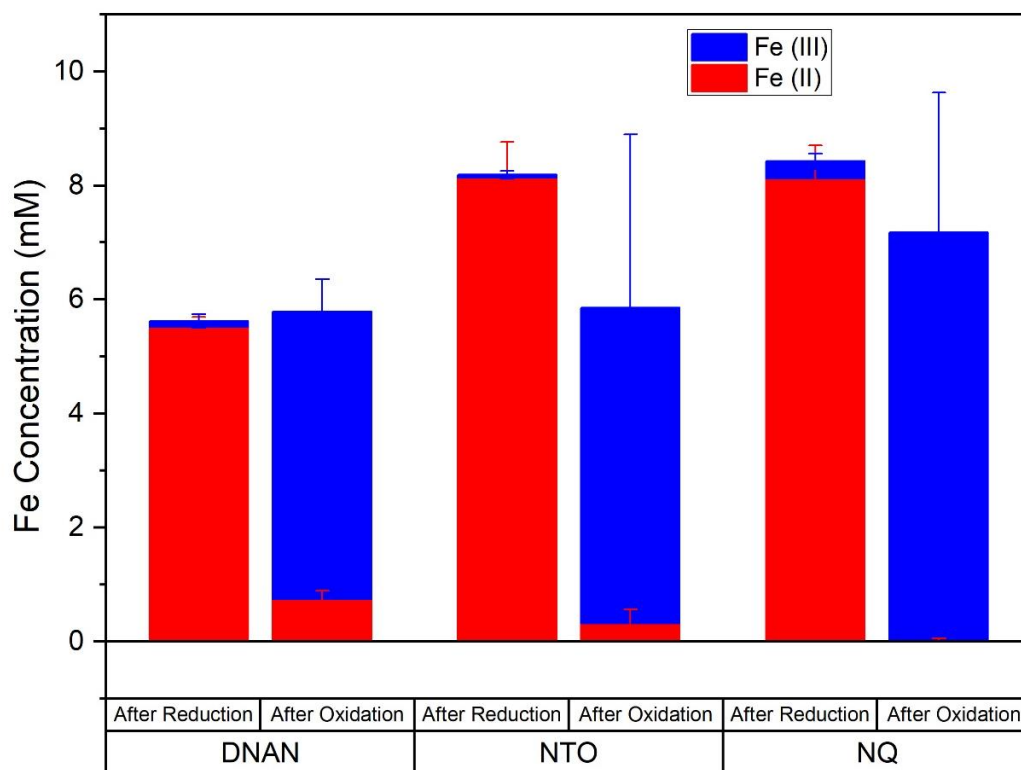


Figure A4 Aqueous Fe(II) and Fe(III) concentrations after reduction and oxidation of three MCs individually. Reaction times were 10 min for reduction and 20 min for oxidation. pH was  $2.0 \pm 0.4$ . Error bars are based on duplicate reactors. Visible precipitates were observed in some reactors after oxidation, which will be Fe(III)-minerals. This would affect the actual amount of aqueous Fe(III) in solution after oxidation.

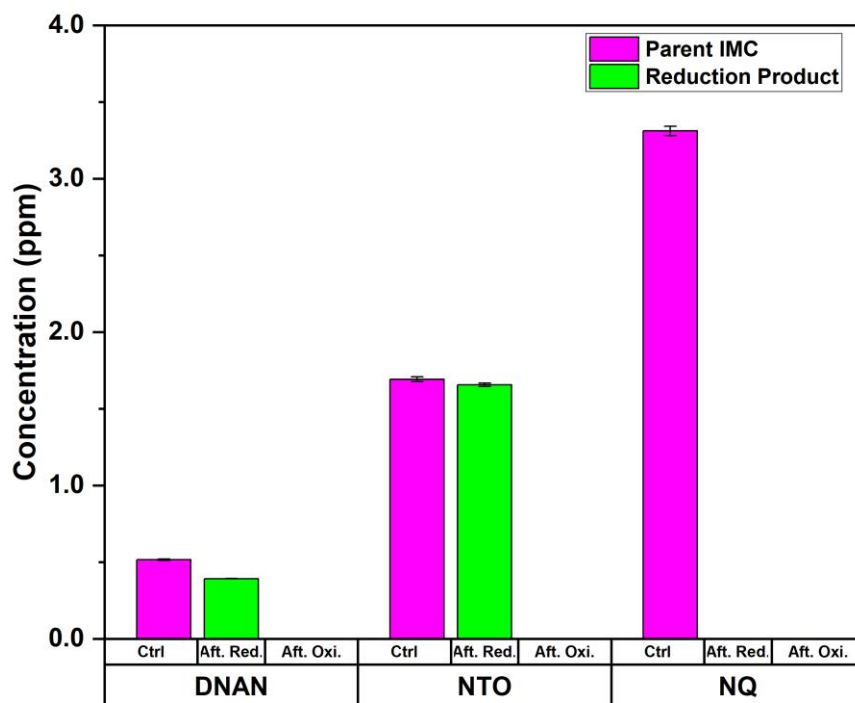


Figure A5 DNAN (0.5 mM), NTO (1.75 mM), and NQ (3.5 mM) and their reduction products (DAAN and ATO, green bars) in synthetic wastewater before reduction (Ctrl), after reduction by nZVI (Aft. Red.), and after oxidation following H<sub>2</sub>O<sub>2</sub> addition (Aft. Oxi.). pH was 2.0±0.4. Error bars are based on duplicate reactors.